About Measurement of PET Spatial Resolution

Martin A. Lodge, John J. Sunderland, and Arman Rahmim, *Senior Member, IEEE*

***Abstract*—Spatial resolution is an important parameter for assessing the performance of positron emission tomography (PET) systems but this apparently simple measurement is complicated by various issues including the reconstruction algorithm, parameter settings and acquisition methodology. Here we describe a series of experiments that aim to untangle some of these issues. Measurements of PET spatial resolution were made using 3 different experimental arrangements: (1) a point source in air; (2) a point source in a radioactive background; and (3) a uniform cylinder positioned at a slightly oblique angle, allowing spatial resolution to be measured from the phantom edge response function. All experiments involved ^{18}F and were performed on a clinical scanner, Biograph mCT. Ordered-subsets expectation maximization including time-of-flight (OSEM+TOF, no point spread function modelling) rapidly converged to a stable full-width at half-maximum (FWHM) for all 3 geometries. OSEM+TOF provided better spatial resolution than Fourier rebinning plus filtered back-projection (FORE+FBP). FWHM degraded with increasing radial distance but in a complex way, apparently dependent on the reconstruction algorithm. FWHM derived from point sources and OSEM+TOF were similar with or without a radioactive background (radial FWHM at 10 cm, 4.77 ± 0.11 mm vs. 4.78 ± 0.06 mm). A uniform cylinder positioned at an oblique angle allowed measurements of radial FWHM (4.74 ± 0.17 mm) that were very consistent with point source measurements. These results support use of the uniform cylinder phantom as a tool for resolution assessment that may be particularly useful for multi-center evaluations due to its simple set-up.**

I. Introduction

SPATIAL resolution is an important parameter for assessing the performance of positron emission tomography (PET) systems but this apparently simple measurement is not as straightforward as it might first seem. Difficulties related to the experimental arrangement, the reconstruction algorithm and parameter settings are just some of the variables that complicate resolution assessment. Here we describe a series of experiments that aim to untangle some of these issues. While we recognize numerous similar experiments have been previously reported and our own measurements are far from complete, the present study addresses important questions regarding the experimental arrangement and image reconstruction. Specifically we compare results from a conventional point source technique with those from a novel, highly practical technique involving an obliquely positioned uniform cylinder phantom.

II. Methods

Measurements of PET spatial resolution were made using 3 different experimental arrangements. Each of the 3 experiments were repeated 3 times on different days and the results were averaged. All data were acquired on a Biograph mCT.

A. Point source in air

An ^{18}F point source was prepared using a small glass capillary tube with activity extending ~1 mm in all directions [1]. The source was supported so as to provide minimal photon attenuation and positioned at various locations within the field-of-view.

B. Point source in water

A similar ^{18}F point source was mounted at the center of a 20 cm diameter, 20 cm long cylinder phantom. The body of the phantom was filled with an aqueous solution of ^{18}F so as to surround the point source with a non-zero background. Different insert-to-background concentration ratios were prepared over 3 separate experiments. The phantom was positioned such that the point source was located in the central slice, 10 cm from the center of the field-of-view.

C. Uniform cylinder at oblique angle

A 20 cm diameter uniform cylinder phantom was filled with ^{18}F and positioned in the center of the field-of-view, at a slightly oblique angle with respect to the *z*-axis (Fig. 1A). Spatial resolution was measured from line profiles across the edges of the phantom [2]. This method incorporating oblique positioning of the phantom has practical advantages over our earlier method [3], [4].

D. Image reconstruction

Images were reconstructed using both ordered-subsets

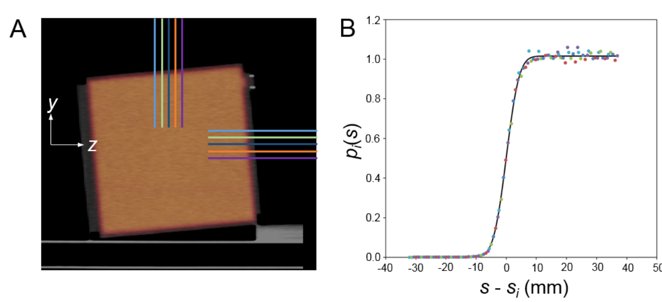

Fig. 1. (A) A uniform cylinder positioned at an oblique angle shown in sagittal orientation. (B) Line profiles across the phantom edge in the *y*-direction allow measurement of the radial component of spatial resolution. The oblique angle allows for very fine sampling of the edge spread function, $p_i(s)$, when multiple slices are combined.

Submitted on December 11, 2018.

M. A. Lodge is with Johns Hopkins University, Baltimore, MD 21287, USA (e-mail: mlodge1@jhmi.edu).

J. J. Sunderland is with the University of Iowa, Iowa City, IA 52242, USA (email: john-sunderland@uiowa.edu).

A. Rahmim is with the University of British Columbia, Vancouver, BC V5Z 1M9, Canada (e-mail: arman.rahmim@ubc.ca)

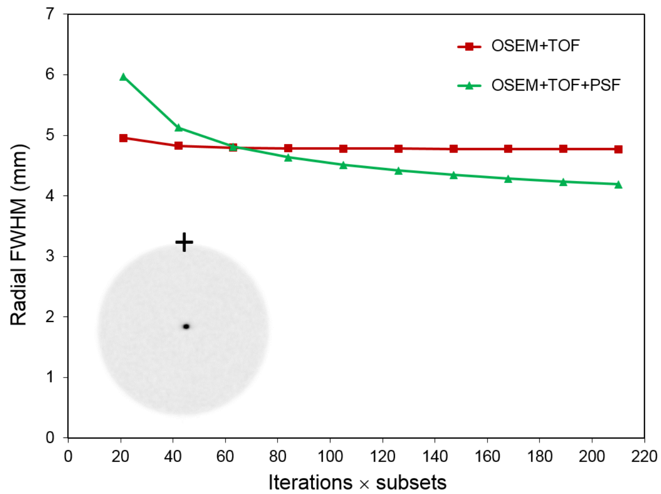

Fig. 2. Spatial resolution (radial component) measured using a point source in a radioactive background. The inset image shows the experimental arrangement with the center of the field-of-view indicated by a cross. Data are shown for OSEM+TOF and also OSEM+TOF+PSF.

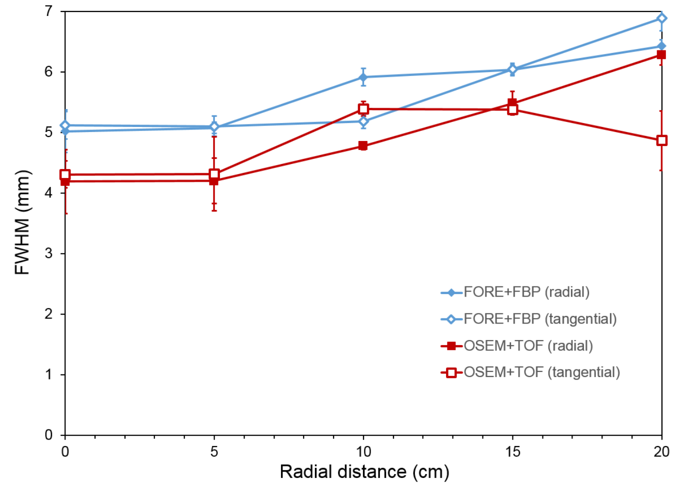

Fig. 3. Spatial resolution derived from in-air point source measurements at various distances from the center of the field-of-view. Results with FORE+FBP and OSEM+TOF (2 iterations) are shown for both radial and tangential directions.

expectation-maximization (OSEM) and Fourier rebinning in conjunction with filtered back-projection (FORE+FBP). OSEM was a fully 3D implementation incorporating time-of-flight (TOF) information, 21 subsets and multiple iterations (n=1…10). Point spread function modeling (PSF) was not included except where noted. FORE+FBP incorporated unapodized ramp filtering. No post-reconstruction filtering was applied in either case.

E. Data analysis

Full-width at half-maximum (FWHM) was used to characterize spatial resolution and, in the case of the point source experiments, was determined using linear interpolation. For the uniform cylinder, the oblique positioning of the phantom allowed for very fine sampling of the edge spread function when line profiles from different locations were combined (Fig. 1B). Radial FWHM was determined by fitting a model to the composite edge profile, under the assumption of a Gaussian response function.

III. Results

A. Convergence

OSEM+TOF reconstruction rapidly converged and beyond a certain point, the FWHM did not change greatly with increasing iterations (Fig. 2). For the in-air point source experiments, convergence was reached within ~20 updates. For the more complex in-water point source and uniform cylinder distributions, convergence was reached within ~40-60 updates. Fig. 2 also shows data from additional reconstructions incorporating PSF and it can be seen that these data did not converge over the range of iterations.

B. Reconstruction algorithm

OSEM+TOF tended to give better spatial resolution than FORE+FBP. For example, in-air point sources at the center of the field-of-view had FWHMs of 4.25 ± 0.37 with OSEM+TOF (2 iterations) and 5.07 ± 0.27 mm with FORE+FBP.

C. Dependence on radial distance

FWHM derived using in-air point sources degraded with increasing distance from the center of the field-of-view for both radial and tangential directions (Fig. 3). The radial component was not always worse than the tangential component and appeared to be dependent on the reconstruction algorithm. For example at a distance of 10 cm, radial FWHM > tangential FWHM for FORE+FBP but the opposite was the case when the same projection data were reconstructed with OSEM+TOF. This observation was highly reproducible and was consistent for both in-air and in-water experiments.

D. Comparison of in-air and in-water point sources

FWHM derived from in-air and in-water point sources were very similar. For OSEM+TOF (2 iterations) at a distance of 10 cm, radial FWHM was 4.78 ± 0.06 and 4.77 ± 0.11 mm for in-air and in-water experiments respectively. At the same location, tangential FWHM was 5.39 ± 0.12 and 5.37 ± 0.22 mm for in-air and in-water experiments. In-water FWHM was measured over a range of insert-to-background ratios from 7-to-1 to 26-to-1 (image ratio as opposed to real concentration ratio).

E. Comparison of measurement geometries

The edge of the uniform cylinder measured spatial resolution in the radial direction at a distance of 10 cm from the center of the field-of-view. With OSEM+TOF (2 iterations) the FWHM was 4.74 ± 0.17 mm which was very consistent with the corresponding point source measurements in-air (4.78 ± 0.06 mm) and in-water (4.77 ± 0.11 mm).

IV. Discussion

Numerous acquisition and reconstruction combinations are feasible and this study has considered only a fraction of the relevant conditions. Nevertheless this series of measurements suggest various interesting possibilities: (1) Point source measurements are not greatly dependent on iterations when using OSEM+TOF; (2) OSEM+TOF provides better spatial resolution than FORE+FBP, possibly because of a more accurate system model; (3) FWHM degraded with increasing radial distance, most probably due to greater inter-crystal penetration but the behavior also seemed to be influenced by other factors such as the reconstruction algorithm; (4) FWHM derived from point sources and OSEM+TOF were similar with or without a radioactive background; (5) A uniform cylinder positioned at an oblique angle allows measurements of FWHM that are very consistent with point source measurements.

V. Conclusion

Spatial resolution derived from iterative reconstruction (without PSF) rapidly converged to a stable FWHM and was very consistent for 3 different experimental arrangements. These results support use of the uniform cylinder phantom as a tool for resolution assessment that may be particularly useful for multi-center evaluations due to its simple set-up.

References

[1] Performance measurements of positron emission tomographs, NEMA NU 2-2012.

[2] M. A Lodge, J. P. Leal, A. Rahmim, J. J. Sunderland and E. C. Frey, “Measuring PET spatial resolution using a cylinder phantom positioned at an oblique angle,” J. Nucl. Med., vol. 59, no. 11, pp. 1768-1775, Nov. 2018.

[3] M. A. Lodge, A. Rahmim and R. L. Wahl, “A practical, automated quality assurance method for measuring spatial resolution in PET,” J. Nucl. Med., vol. 50, no. 8, pp. 1307-1314, Aug. 2009.

[4] M. A. Lodge, A. Rahmim and R. L. Wahl, “Simultaneous measurement of noise and spatial resolution in PET phantom images,” Phys. Med. Biol., vol. 55, no. 4, pp. 1069-1081, Jan. 2010.